The MYC Oncogene Cooperates with Sterol Regulated Element-Binding Protein To Regulate Lipogenesis Essential for Neoplastic Growth

Supplementary Information

Arvin M. Gouw[a*], Katherine Margulis[b*], Natalie S. Liu[a], Sudha J. Raman[c], Anthony Mancuso[d], Georgia G. Toal[a], Ling Tong[a], Adriane Mosley[a], Annie L. Hsieh[d] , Delaney K. Sullivan[a], Zachary E. Stine[d], Brian J. Altman[d], Almut Schulze[c], Chi V. Dang[d,e,f**],
Richard N. Zare[b**], Dean W. Felsher[a**]

Affiliations

[a]Division of Oncology, Departments of Medicine and Pathology, Stanford University School of Medicine, Stanford, CA 94305, USA

[b]Department of Chemistry, Stanford University, Stanford, CA 94305, USA

[c]Departments of Biochemistry and Molecular Biology, Wurzburg University, Germany.

[d]Departments of Medicine, Abramson Family Cancer Research Institute, Perelman School of Medicine, University of Pennsylvania, Philadelphia, PA 19104, USA

[e]Ludwig Institute for Cancer Research, New York, NY 10017, USA

[f]The Wistar Institute, Philadelphia, PA 19104, USA

*These authors contributed equally to this work, and either has the right to list himself first in bibliographic documents

**To whom correspondence should be addressed; email: dfelsher@stanford.edu; zare@stanford.edu, cdang@lcr.org

Lead contact: dfelsher@stanford.edu

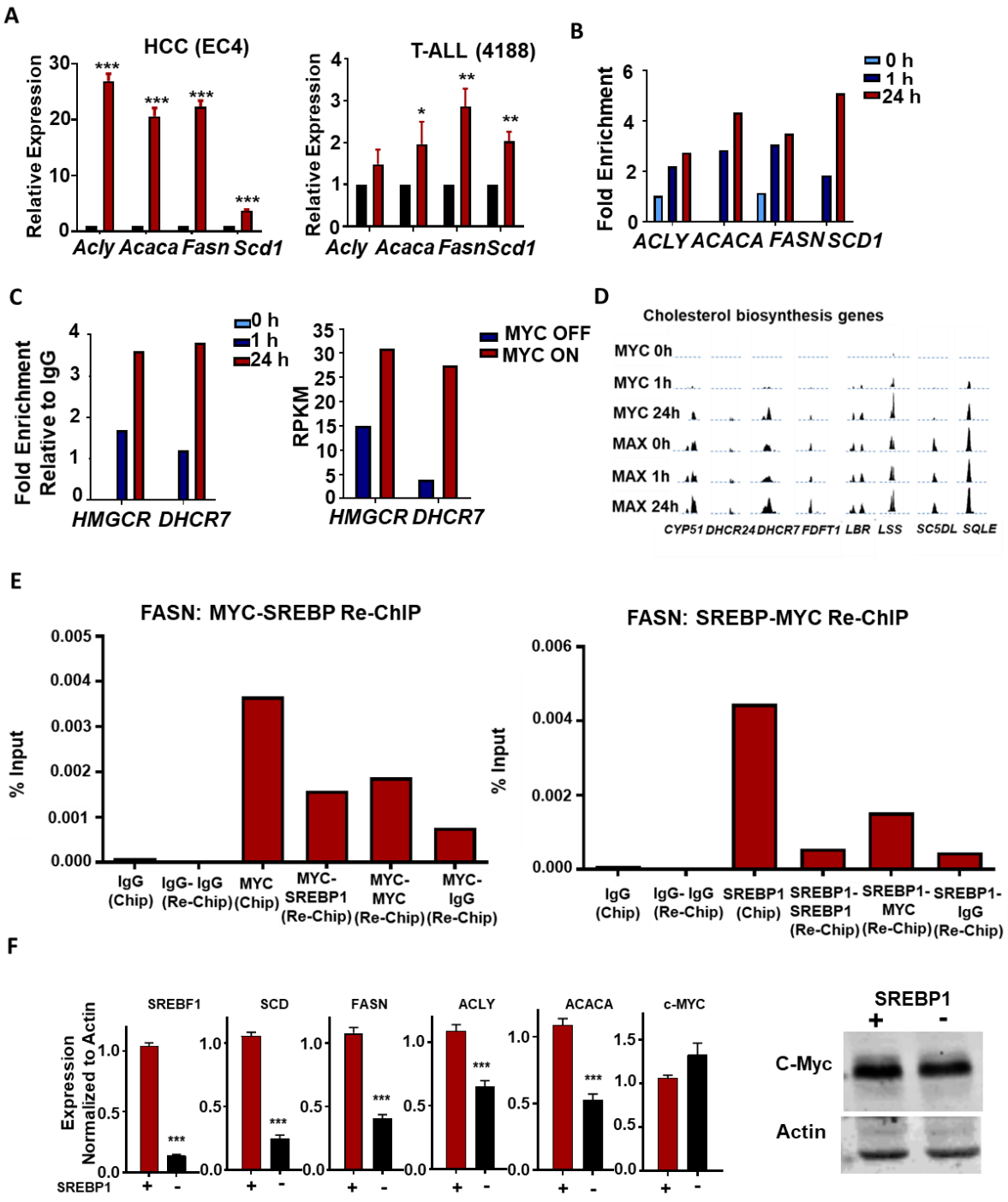

Figure S1. Related to Figures 2, 3, 4. MYC upregulates lipid metabolic genes. (A) qPCR shows fatty acid synthesis mRNA expression in high MYC (red bars, N=3 per cell line) compared to 24 hours of MYC inactivation (black bars, N=3 per cell line) in HCC (EC4) and T-ALL (4188) cell lines. Statistical significance by t-test, **P*<0.05, ***P*<0.01, ****P*<0.001. (B) Binding profile of MYC on fatty acid synthesis genes from publicly available MYC ChIP-Seq in P493-6 cells 0, 1 and 24 hours after

tetracycline release. (C) Fold change of quantification (reads per million) of publicly available MYC ChIP-Seq on cholesterol biosynthesis genes in BCL (P493-6) cells 0, 1 and 24 hours after tetracycline release (left). RNA-seq shows MYC effect on expression of cholesterol biosynthesis genes comparing MYC OFF and 24 hours MYC ON in BCL (P493-6) cells (right). (D) Timecourse binding data of publicly available MYC ChIP-Seq in P493-6 cells 0, 1 and 24 hours after tetracycline release showing MYC and MAX binding on cholesterol biosynthesis genes. (E) MYC and SREBP1 both bind to FA synthesis gene promoters as shown by MYC ChIP with SREBP1 re-ChIP and SREBP1 ChIP with MYC re-ChIP for FASN. (F) Knockdown of SREBP1 lowers FA synthesis genes but not MYC expression by ChIP, indicating that SREBP1 can function independent of MYC (left). Statistical significance by t-test, ***$P<0.001$. Western blot shows that c-Myc level in SREBP1 knockdown are similar to control (right).

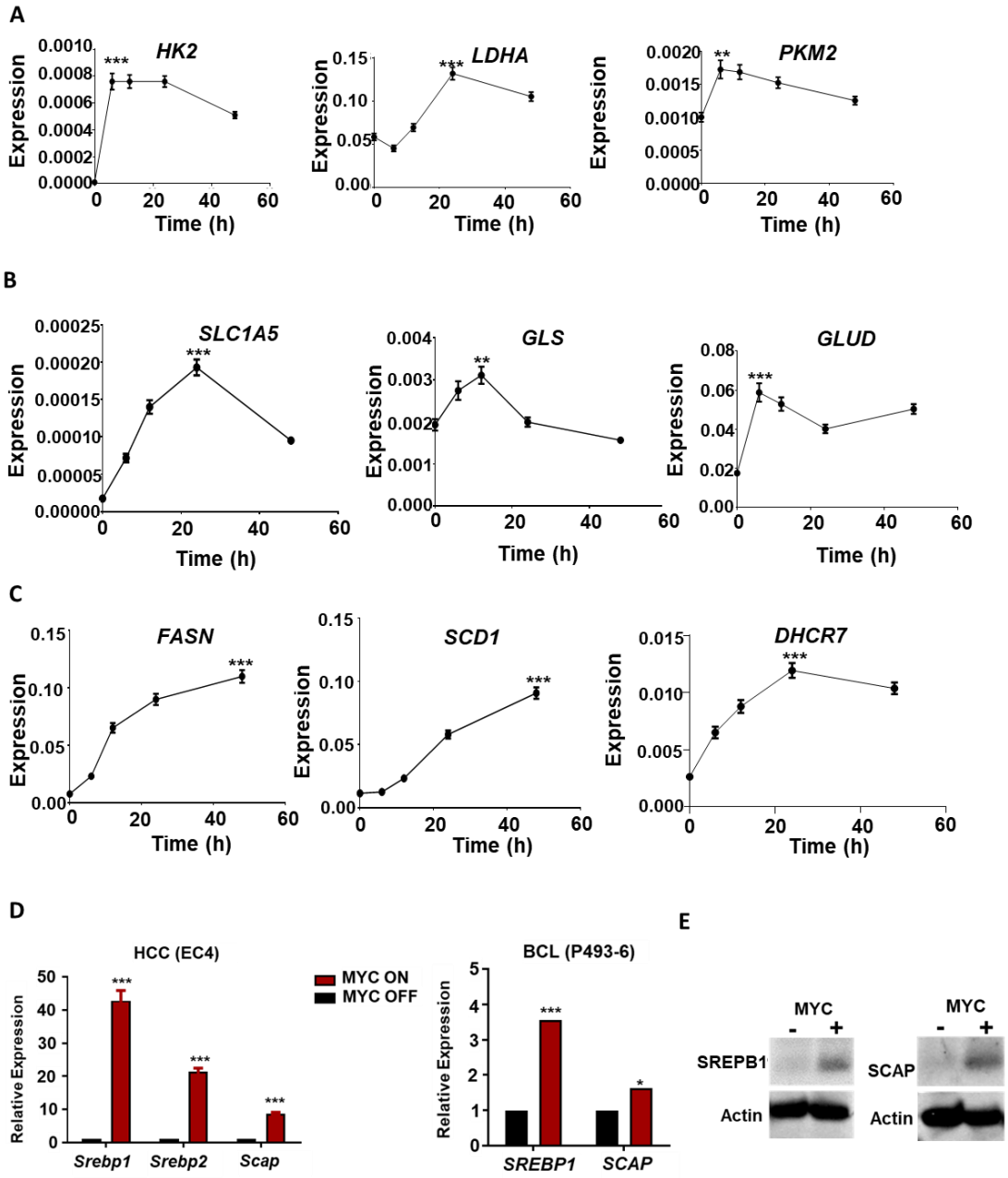

Figure S2. Related to Figures 2, 3, 4. MYC non-linearly induces metabolic genes via induction of Srebp1. (A) Timecourse mRNA levels in BCL (P493-6) cells 0, 6, 12, 24 and 48 hours after tetracycline release of glycolysis genes, (B) glutaminolysis genes, and (C) fatty acid and cholesterol synthesis genes. (D) qPCR shows mRNA relative expression of both *Srebp* and *Scap* in murine HCC line EC4 (N=3) (left) and in human BCL line P493-6 (N=3) (right). Statistical significance by t-test, **P*<0.05, ***P*<0.01, ****P*<0.001. (E) Western blot shows dependence of SREBP1 and SCAP on MYC levels in BCL (P493-6).

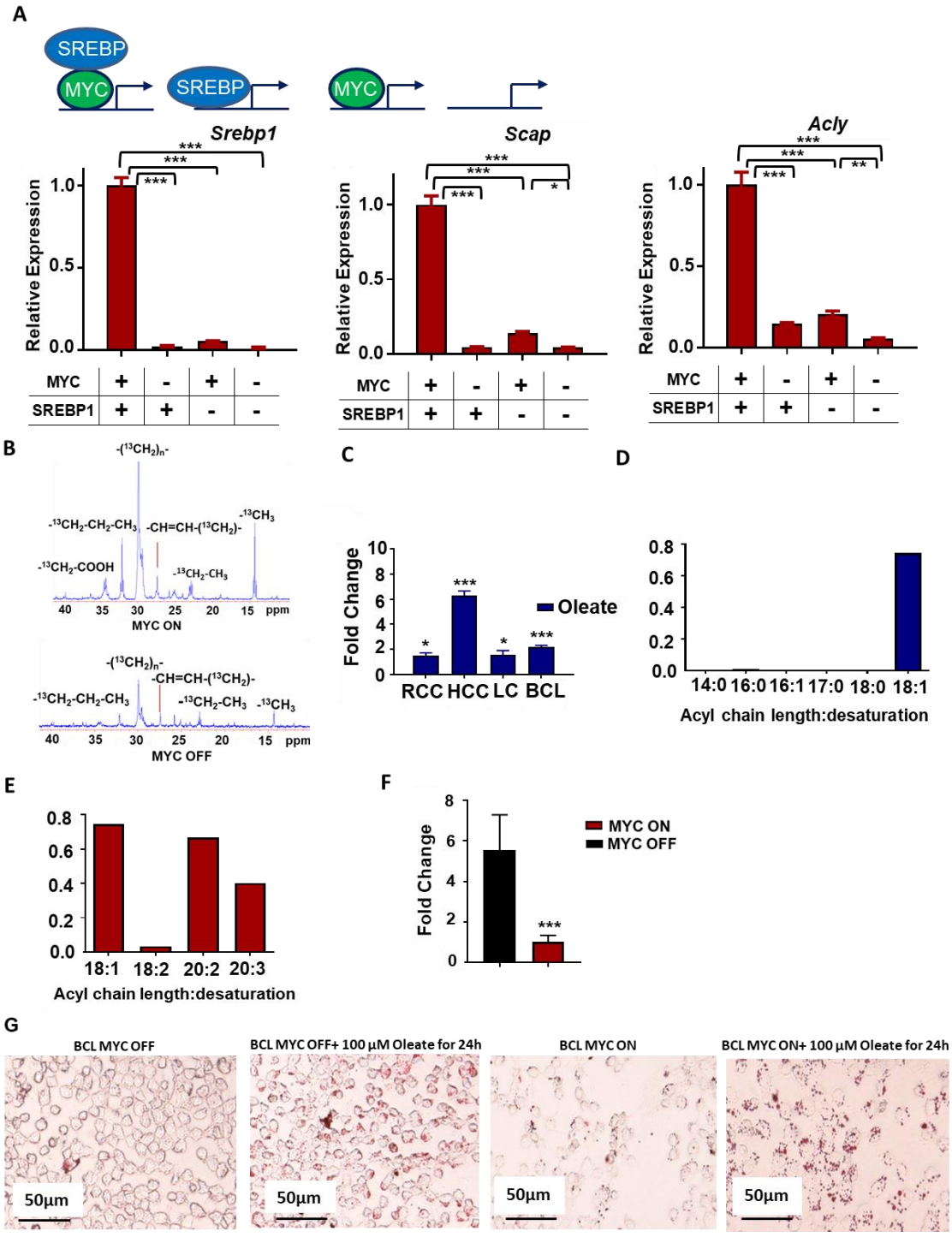

Figure S3. Related to Figures 4, 5. MYC and SREBP1 induce fatty acid synthesis. (A) mRNA expression of *Srebp1*, *Scap*, and *Acly* upon siRNA knockdown of Srebp1 or scramble RNA in HCC (EC4) under MYC ON and OFF conditions (N=3 per condition). Statistical significance by two-way ANOVA using Tukey's multiple comparisons post tests, .**P*<0.05, ***P*<0.01, ****P*<0.001. Overall, ****P*<0.001 for SREBP1

effect, ***P<0.001 for MYC effect and ***P<0.001 for interaction between the two. (B) Close-up look into glucose and glutamine contribution to lipogenesis by NMR in MYC ON (left) *vs* OFF in BCL (P493-6) cells (right). (C) Levels of oleate detected by DESI-MSI in MYC ON relative to MYC OFF in RCC, HCC, LC, and BCL (N=3 per group, per transgenic system). Statistical significance by t-test, *P<0.05, **P<0.01, ***P<0.001. (D)Incorporation of ^{13}C-labeled oleate in MYC ON BCL (P493-6) cells. (E)^{13}C-labeled glucose is converted to fatty acids in MYC ON BCL (P493-6) cells. (F) H^3-palmitate oxidation rate fold change in BCL P493-6 cells in MYC ON state *vs* MYC OFF. N=4. Statistical significance by t-test, ***P<0.001. (G)Oleate droplets containing red dye are metabolized in MYC OFF BCL and stored unchanged in MYC ON BCL.

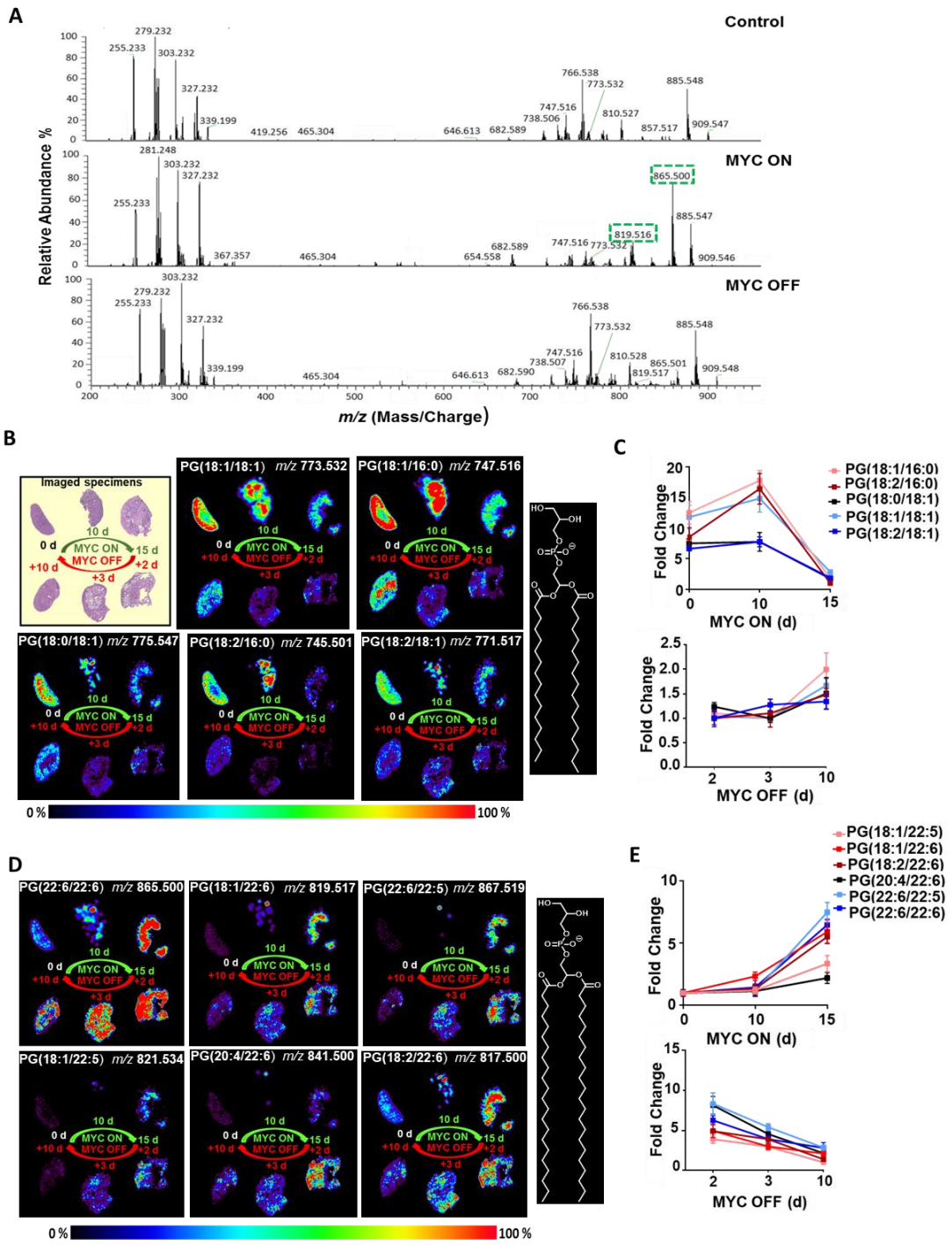

Figure S4. Related to Figures 5, 6. Dynamic changes of PG profile in RCC by DESI-MSI. (A) Average mass spectra for species in *m/z* range 200-1000 in control kidney, 15 days MYC activation (MYC ON), and subsequent 10 days MYC inactivation (MYC OFF). (B) Representative DESI-MSI distribution of short acyl chain PGs with H&E staining of the tissues following 15 days MYC activation and 10 days MYC inactivation. General molecular structure of these phospholipids is given in the right panel, and (C) their quantification upon MYC activation (top) and inactivation (bottom), N=3 mice per time point. (D)

Representative DESI-MSI distribution of long acyl chain PGs in RCC following 15 days MYC activation and 10 days MYC inactivation. General molecular structure of these phospholipids is given in the right panel, and (E) their quantification upon MYC activation (top) followed by inactivation (bottom), N=3 mice per time point.

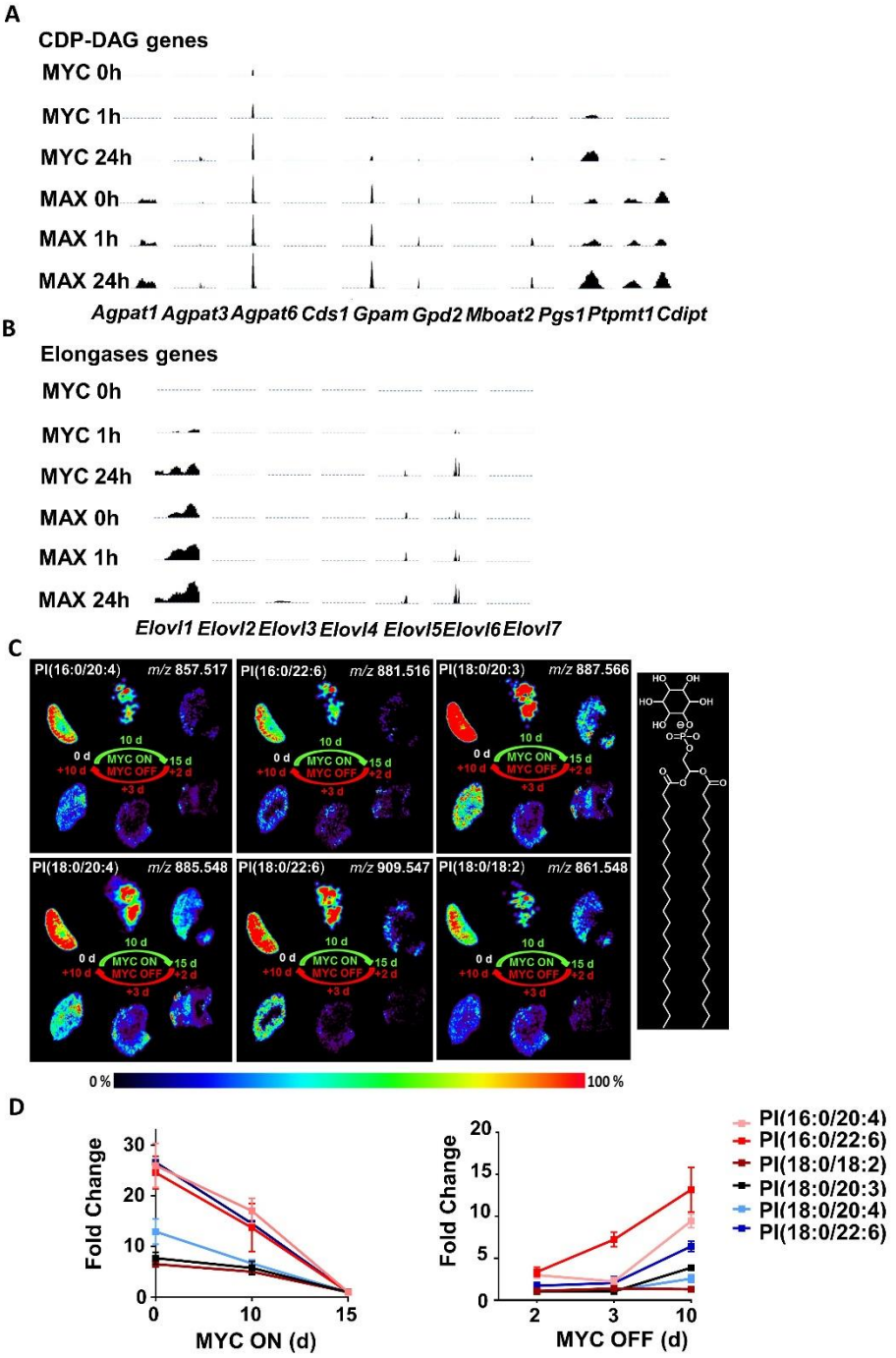

Figure S5. Related to Figures 5, 6. MYC binds to PG synthesis and elongase genes and regulates PIs. Binding data of publicly available MYC and MAX ChIP-Seq in BCL (P493-6) cells 0, 1 and 24 hours after tetracycline release on the promoters of (A) CDP-DAG synthesis genes, and (B) elongases. (C) Representative DESI-MSI distribution of PIs in RCC following 15 days of MYC activation and 10 days of MYC inactivation. Molecular structure of these phospholipids is given in the right panel. (D) Quantification of PIs upon MYC activation (left), and MYC inactivation (right), N=3 mice per time point.

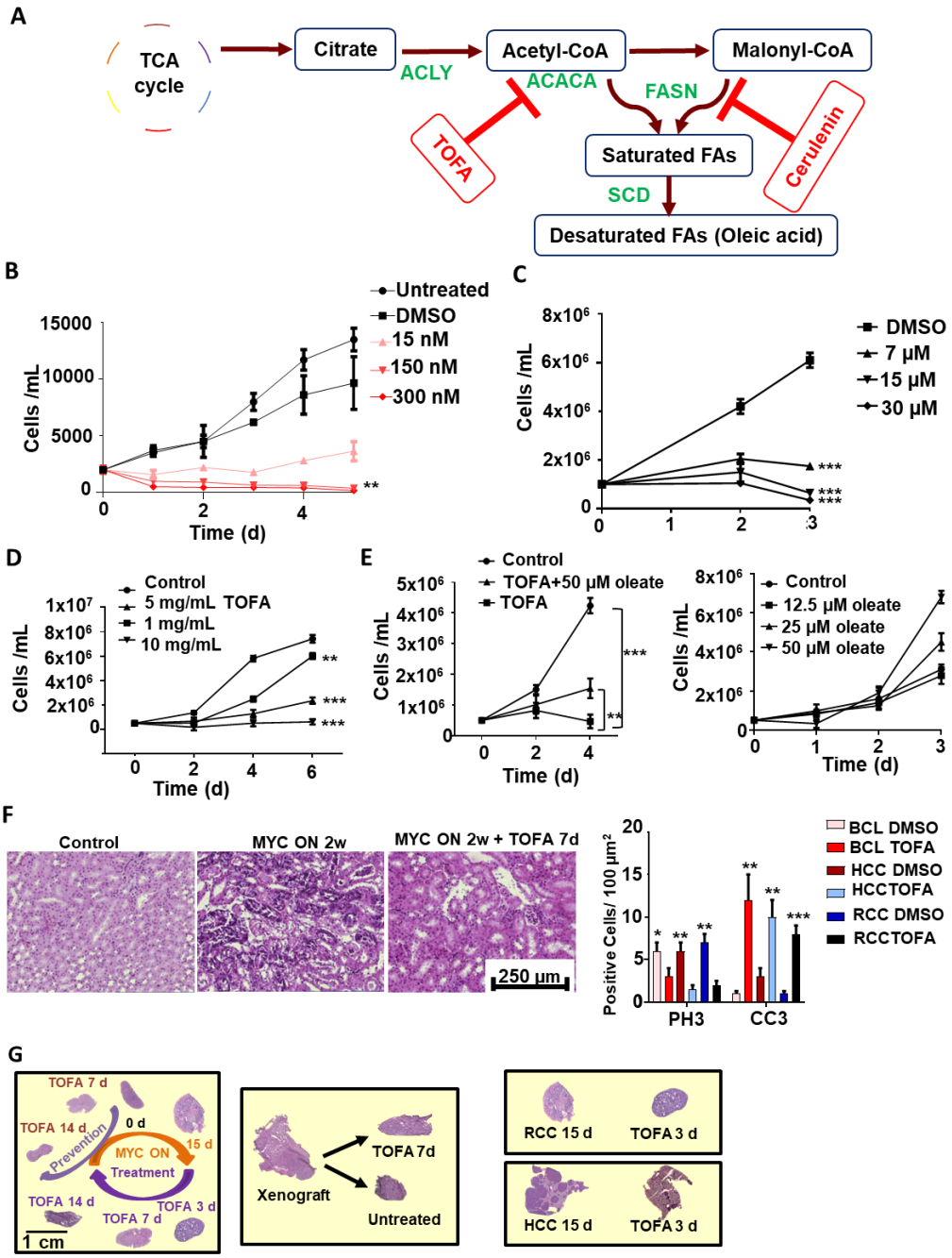

Figure S6. Related to Figures 6, 7. Inhibition of fatty acid synthesis decreases cancer proliferation. (A) Scheme of fatty acid inhibition sites: dose-dependent inhibition of lipogenesis by cerulenin, an FASN inhibitor, and TOFA, an ACACA inhibitor. (B) Dose-dependent administration of cerulenin and BCL (P493-6) proliferation, *in vitro*, N=3. (C) Dose-dependent administration of TOFA and BCL (P493-6) proliferation *in vitro*, N=3. (D) Dose-dependent administration of TOFA and RCC (E28) proliferation, *in vitro*, N=3. (E) Oleate administration along with 5mg/mL TOFA *vs* 5mg/mL TOFA alone *vs* untreated in

RCC (E28) line, *in vitro*, N=3 (left), and oleate dose response curve on RCC (E28) proliferation *in vitro*, N=3 (right). Statistical significance by t-test, $^{**}P<0.01$, $^{***}P<0.001$. (F) H&E of mouse RCC kidney in wild-type, MYC ON untreated, and TOFA-treated for 7 days after MYC induction for 2 weeks (on the left) and quantification of cellular death by immunohistochemical staining of proliferation marker phosphor-histone 3 (PH3), apoptotic marker cleaved caspase 3 (CC3) in mouse RCC, human BCL, and mouse HCC after ACACA inhibition with TOFA (N=3 per group). (G) H&E stained tissues shown in DESI-MS images.

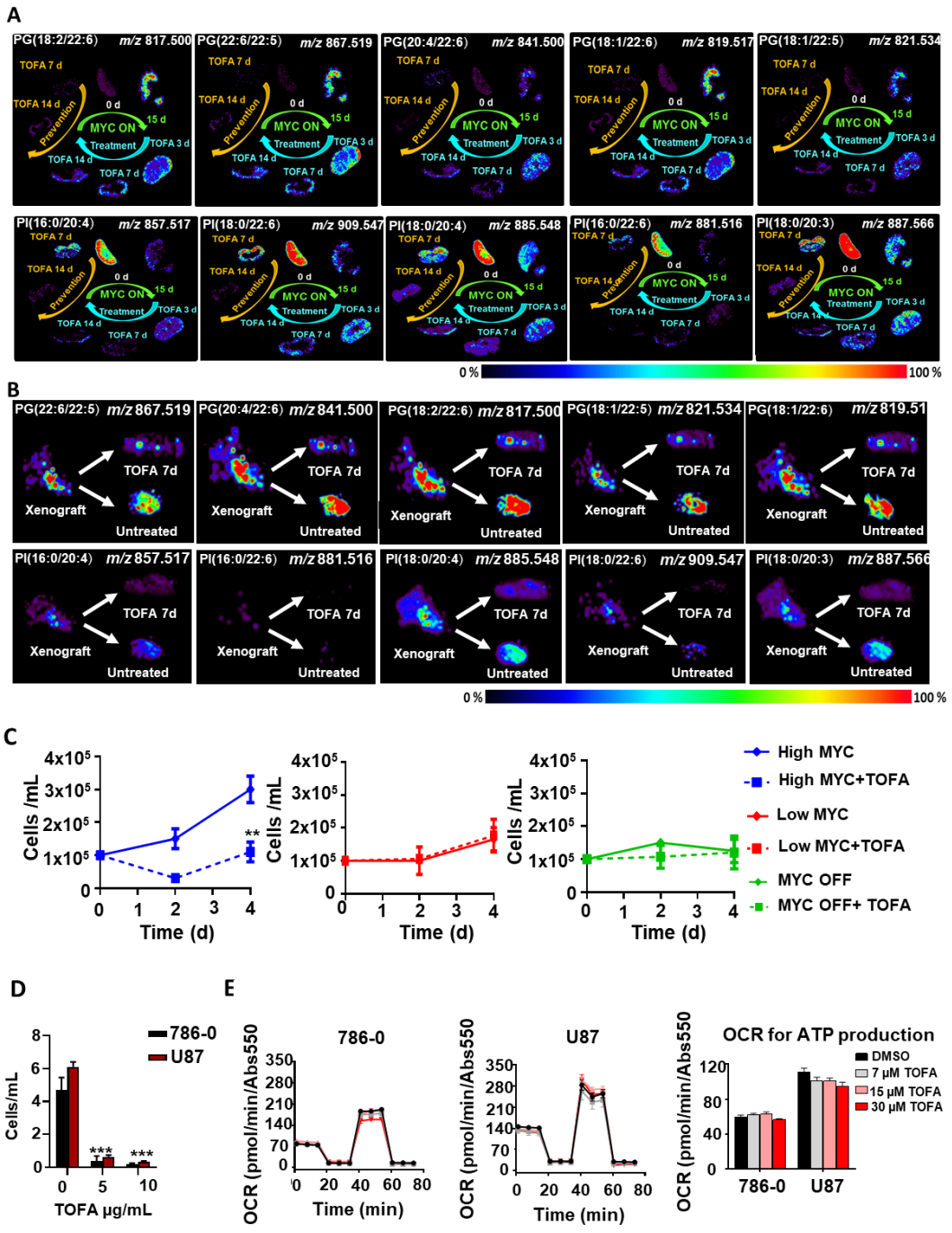

Figure S7. Related to Figures 6, 7. TOFA treatment and prevention tumors. (A) Representative distribution of PGs and PIs in murine RCC model upon TOFA treatment of 15-day MYC-induced tumor and prevention at day 0 of MYC induction. (B) Representative distribution of PGs and PIs upon TOFA treatment for 7 days of 15-day human RCC 786-0 subcutaneous xenografts in NSG mice. (C) Cell proliferation inhibition by TOFA in BCL (P493-6) at various MYC levels controlled by low/ high dose DOX addition. High MYC cells were treated with 0ng/mL doxycycline, low MYC with 0.2ng/mL, MYC

OFF with 2ng/mL. Statistical significance by t-test, $^{**}P<0.01$. (D) Sensitivity of human RCC (786-0) and human glioblastoma (U87) cell lines to TOFA inhibition achieved by 5 and 10 μg/mL TOFA addition for 3 days *vs* control. Statistical significance by t-test, $^{***}P<0.001$. (E) Oxygen consumption rate of human RCC cell line (786-0) (left panel) and human glioblastoma (U87) cell lines (middle panel) before and after TOFA treatment. Oxygen consumption rates for ATP production for both cell lines are shown in the right panel after addition of various doses of TOFA.

Table S1. Related to Figures 5, 6. Tandem mass spectrometry data used for identification of molecular ions

Measured *m/z*	**Main Fragment Ions**	**Tentative attribution[a]**	**Exact *m/z***	**Mass error[b] (ppm)**	**Proposed formula[c]**
745.5004	391.22, 279.23, 255.23	PG(18:2/16:0)	745.5025	-2.0	$C_{40}H_{74}O_{10}P$
747.5159	491.28, 465.26, 483.27, 391.23, 281.25, 255.23	PG(18:1/16:0)	747.5182	-3.1	$C_{40}H_{76}O_{10}P$
771.5157	489.26, 415.22, 281.25, 279. 23	PG(18:1/18:2)	771.5182	-3.2	$C_{42}H_{76}O_{10}P$
773.5315	509.29, 417.24, 281.25	PG(18:1/18:1)	773.5338	-3.0	$C_{42}H_{78}O_{10}P$
775.5485	493.29, 419.26, 281.25, 283.26	PG(18:1/18:0)	775.5495	-1.3	$C_{42}H_{80}O_{10}P$
817.5006	327.23, 283.24, 279.23	PG(18:2/22:6)	817.5025	-2.3	$C_{46}H_{74}O_{10}P$
819.5163	555.27, 537.26, 463.22, 327.23, 283.24, 281.24	PG(18:1/22:6)	819.5182	-2.3	$C_{46}H_{76}O_{10}P$
821.5307	465.24, 329.25, 281.25	PG(18:1/22:5)	821.5338	-3.8	$C_{46}H_{78}O_{10}P$
841.5004	327.23, 303.23, 283.24	PG(20:4/22:6)	841.5025	-2.5	$C_{48}H_{74}O_{10}P$
865.5006	555.27, 537.26, 463.22 327.23, 283.24	PG(22:6/22:6)	865.5025	-2.1	$C_{50}H_{74}O_{10}P$
867.5170	555.27, 329.25, 327.23, 285.26, 283.24	PG(22:6/22:5)	867.5182	-1.4	$C_{50}H_{76}O_{10}P$
857.5158	601.28, 571.29, 553.28, 391.22, 303.22, 255.23	PI(16:0/20:4)	857.5186	-3.3	$C_{45}H_{78}O_{13}P$
861.5479	599.32, 581.31, 419.26, 297.04, 283.26	PI(18:0/18:2)	861.5499	-2.3	$C_{45}H_{82}O_{13}P$
881.5162	625.28, 571.29, 553.28, 463.23, 391.22, 327.23	PI(16:0/22:6)	881.5186	-2.7	$C_{47}H_{78}O_{13}P$

885.5475	599.32, 581.31, 439.22, 419.26, 303.23, 283.26	PI(18:0/20:4)	885.5499	-2.7	$C_{47}H_{82}O_{13}P$
887.5657	603.29, 599.32, 581.31, 441.24, 437.26, 419.26, 305.25, 283.26	PI(18:0/20:3)	887.5655	0.2	$C_{47}H_{84}O_{13}P$
909.5474	625.28, 599.32, 581.31, 463.23, 419.27, 327.23, 297.04, 283.24	PI(18:0/22:6)	909.5499	-2.7	$C_{49}H_{82}O_{13}P$

[a] FA = fatty acids, PG = glycerophosphoglycerols; (X:Y) denotes the total number of carbons and double bonds in the fatty acid chains. The most abundant isomer based on the fragments is listed.

[b] Mass errors were calculated based on the exact monoisotopic *m/z* of the deprotonated form of the assigned molecules.

[c] Proposed formula for the deprotonated molecular ion detected.